Defect states in hybrid solar cells consisting of Sb_2S_3 quantum dots and TiO_2 nanoparticles

Dong Uk Lee, Sang Woo Pak, Seong Gook Cho, Eun Kyu Kim' , and Sang Il Seok

Citation: Appl. Phys. Lett. **103**, 023901 (2013); doi: 10.1063/1.4813272

View online: http://dx.doi.org/10.1063/1.4813272

View Table of Contents: http://aip.scitation.org/toc/apl/103/2

Published by the American Institute of Physics

Defect states in hybrid solar cells consisting of Sb_2S_3 quantum dots and TiO_2 nanoparticles

Dong Uk Lee,[1] Sang Woo Pak,[1] Seong Gook Cho,[1] Eun Kyu Kim,[1,a)] and Sang Il Seok[2,3]
[1]*Department of Physics and Quantum Function Research Laboratory, Hanyang University, Seoul 133-791, South Korea*
[2]*Division of Advanced Materials, Korea Research Institute of Chemical Technology, 141 Gajeong-Ro, Yuseong-Gu, Daejeon 305-600, South Korea*
[3]*Department of Energy Science, Sungkyunkwan University, Suwon 440-746, South Korea*

(Received 9 April 2013; accepted 19 June 2013; published online 8 July 2013)

We have studied defect states in an organic-inorganic hybrid solar cell containing Sb_2S_3 quantum dots (QDs) and TiO_2 nanoparticles (NPs) by using deep level transient spectroscopy (DLTS). An Au electrode was deposited as a Schottky contact on the sample, where the Sb_2S_3 QDs were distributed on the surface of TiO_2 NPs by chemical synthesis. The activation energy and capture-cross section of an interface state between the Sb_2S_3 QDs and the TiO_2 NPs were found to be about 0.78 eV and 2.21×10^{-9} cm^{-2}, respectively. Also, the densities of this interface trap under a measurement voltage of -1 V were approximately 2.5×10^{17} cm^{-3}. Based on these results, the interface trap was positioned around $E_c - 1.03$ eV below the conduction band edge of Sb_2S_3 QD. Thus, the external quantum efficiency of the solar cell was affected because of its role as a recombination center for carriers generated from Sb_2S_3 QDs. © *2013 AIP Publishing LLC*.
[http://dx.doi.org/10.1063/1.4813272]

Solar cells based on quantum dots (QDs) may represent a breakthrough technology for next-generation solar devices. Crystalline Sb_2S_3 is one of the most promising semiconductor materials for photovoltaic cells because of its high absorption coefficient and optimum bandgap. To enhance quantum efficiency for applications in organic-inorganic heterojunction solar cells with semiconductor QDs, a variety of things should be investigated, including defect states and the interface states among the QDs, the conducting carrier transportation layer, and the metal electrode layer.[1–6] To optimize the electrical properties of hybrid organic-inorganic solar cells with semiconductor QDs, the defect states in the solar cell structures have been studied in terms of their origins and energy states. Recently, QD solar cells have been investigated to improve the external quantum efficiency through modulation of band aliment between the QDs and the electron and the hole-conducting layer. It was reported that the efficiency of a hybrid QD solar cell depends on the transportation speed of generated excitons before the recombination of carriers in the semiconductor layer.[7–11] In general, interface traps in a QD solar cell can reduce the external quantum efficiency by recombination of the separated carriers.

In this letter, the defect states in a hybrid solar cell consisting of Sb_2S_3 QDs and TiO_2 nanoparticles (NPs) were investigated using deep level transient spectroscopy (DLTS). Then, the electrical properties, such as density, cross-section, and activation energy for the interface state between the Sb_2S_3 QDs and the TiO_2 NPs were determined. We further discussed the effect of the interface state on the quantum efficiency of the semiconductor QD solar cell.

The fabrication process of hybrid QD solar cells using Pilkington TEC-15 conducting transparent glass as substrate was as follows. TiO_2 paste having a diameter of about 60 nm for TiO_2 NPs (NPs) was synthesized by hydrothermal treatment at 250 °C for 12 h by using a peroxotitanium complex solution. Also, a dense TiO_2 thin film was deposited by spray pyrolysis on the fluorine-doped tin oxide (FTO) glass substrate. The TiO_2 NPs were screen-printed on the dense TiO_2 thin film using paste and were subsequently sintered at 500 °C for 30 min. The samples were then soaked in a $TiCl_4$ solution for 12 h and then sintered at 500 °C for 30 min after cleaning with deionized water and ethanol. Finally, the Sb_2S_3 QDs were deposited onto the surface of TiO_2 NPs formed on the FTO layer by chemical bath deposition, which provides high surface coverage and strong anchoring to the electrode.[12–14] Samples were then annealed at 330 °C for 30 min in an Ar atmosphere.

To investigate the defect states of Sb_2S_3 QDs, an Au electrode was deposited by using a thermal evaporator such that the diameter and thickness were 300 μm and 200 nm, respectively. The sample structure consisting of Au Schottky contact /Sb_2S_3 QDs/TiO_2 NPs/FTO layer/glass is shown in Fig. 1. The interface states in the Sb_2S_3 QDs for solar cell samples were measured by means of a DLTS system, which consisted of HP4280A and Boonton 7200 capacitance meters, a HP8116A pulse generator, a SR 640 low-pass filter, a data acquisition system, a Lakeshare 331 temperature controller and a cryostat (12–700 K). Also, the photoluminance (PL) was measured to verify the energy band gap for photon absorbance using a Nd-YAG laser (325 nm and 488 nm).

In the schematic device structure for DLTS measurements of Fig. 1, Sb_2S_3 QDs were distributed on the surface of TiO_2 NPs to allow for the generation of electron-hole pairs as excitons. In this case, the metal layer for the Au Schottky contact was directly deposited on the Sb_2S_3 QDs on TiO_2 NPs without the insulator layer. In order to measure

a)Author to whom correspondence should be addressed. Electronic mail: ek-kim@hanyang.ac.kr

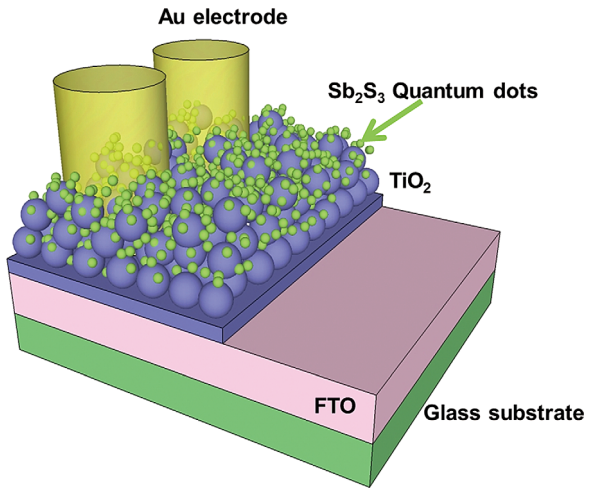

FIG. 1. Three-dimensional schematics of a sample structure with Au electrode/Sb_2S_3 QDs/TiO_2 NP/FTO layers on the glass substrate.

DLTS spectra, a depletion region in the semiconductor layer created by the Schottky contact was required. The depletion behavior of the Sb_2S_3 QD semiconductor was confirmed by measurements using the 1-MHz capacitance-voltage (C-V) sweeping method, as shown in Fig. 2(a), where sweeping voltages were applied from 4 V to −4 V. The shifted flat band of the C-V curve was observed at 300 K; this was caused by the size effect of Sb_2S_3 QDs, while the shift in the Fermi level of the composite heterojunction system was a result of charge equilibration between the metallic NPs and semiconductor QDs.[15,16] Furthermore, hysteresis in the C-V curve caused by charge trapping in Sb_2S_3 QDs is also apparent in Fig. 2(a).

Figure 2(b) shows the PL spectra for comparison between the reference sample and the Sb_2S_3 QDs on surface of TiO_2 NPs. The band-gap of the Sb_2S_3 bulk has been reported to be about 1.7 eV. In comparison with the samples composed as FTO layer/glass and TiO_2 NPs/FTO layer/glass, a broad PL spectrum from the sample with Sb_2S_3 QDs appeared strongly in the range from 1.5 eV to 2.5 eV after laser pumping at 325-nm-wavelength. According to these PL spectra, the absorbed photon energies for solar cell devices fabricated with Sb_2S_3 QDs were approximately in the wavelength range from 496 nm to 826 nm because the optical energy band-gap was dependent on the size of the Sb_2S_3 QDs. It was considered that the broad PL spectrum of Sb_2S_3 QDs is originated from their size distribution in the rage of 5∼10 nm diameter. In addition, the interface trap level could affect PL spectrum broadness by the transition between the trap level and band edge in Sb_2S_3 QDs, which were randomly distributed on the surface of TiO_2 NPs.

Figure 3 shows the DLTS spectra for the Schottky contact with and without Sb_2S_3 QDs. The rate window and pulse voltage in the DLTS spectra were 4.06009 s^{-1} and 0 V, respectively. Signal A was observed in the DLTS spectra for

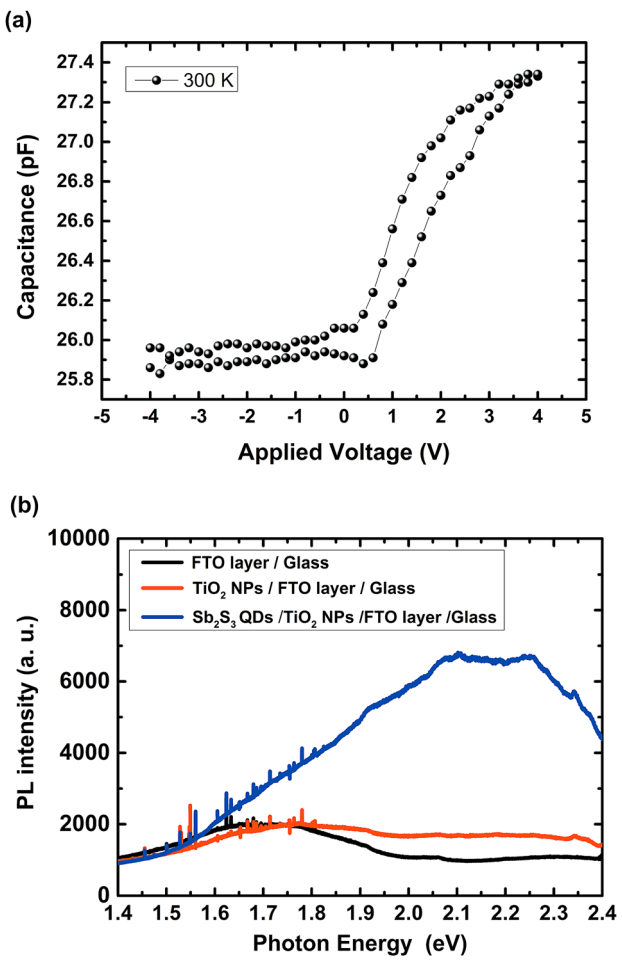

FIG. 2. (a) C-V properties of the device at 300 K, for sweeping voltages applied from 4 V to −4 V and (b) the PL spectra of the samples composed of Sb_2S_3 QDs/TiO_2 NPs /FTO layer/glass substrate, TiO_2 NPs/FTO layer/glass substrate, and the FTO layer/glass substrate.

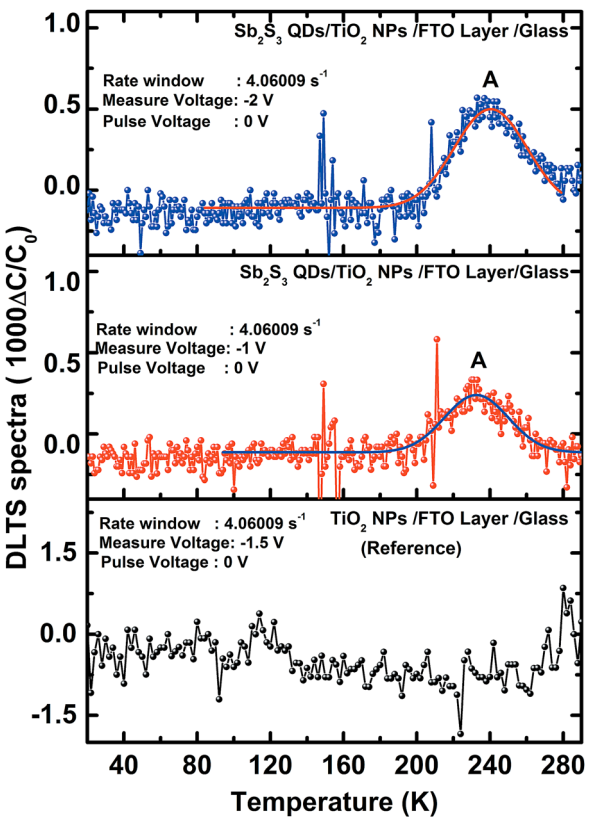

FIG. 3. DLTS spectra with and without the Sb_2S_3 QDs, when the voltages measured after applying a pulse voltage at 0 V were −1.0 V, −1.5 V, and −2.0 V, respectively.

the Sb_2S_3 QDs as a function of temperature from 20 K to 320 K for measured voltages of −2 V and −1 V after a pulse bias applied at 0 V. Here, the DLTS spectra of the reference sample of TiO_2 NPs/FTO layer/glass substrate did not show any signal peaks indicative of carrier trapping. Interestingly, the DLTS spectra of the reference sample also did not show reasonable signals for defect states in TiO_2 NP. Before measuring DLTS spectra, the carrier concentration of the target materials should first be considered. This is important because the length of the depletion region from the Schottky contact on the surface to the semiconductor layer depends on both the carrier concentration in the semiconductor and the work function of the contact material. The noise signals appearing between 140 and 160 K in the DLTS spectra of Sb_2S_3 QDs could be caused by the undefined capacitance-time curve through rapidly decreased capacitance.

An Arrhenius plot for DLTS spectra obtained from solar cells with Sb_2S_3 QDs is shown in Fig. 4. The activation energy for signal A in the DLTS spectra is obtained from the following equation:

$$\log\frac{e_n}{T^2} = \log A_n\sigma_n + \left(-\frac{\Delta E_a \times \log e}{1000\,k}\right)\frac{1000}{T}, \qquad (1)$$

where σ_n is the capture cross section of the trap, k is the Boltzmann constant, m_n^* is the effective mass of the electron and hole, and h is the Planck's constant. Also, the coefficient A_n can be expressed as $4\sqrt{6}\pi^{3/2}k^2m_n^*/h^3$ and $e_n = A_n\sigma_n T^2 \exp(\Delta E_a/kT) = 1/\tau$. The activation energy (ΔE_a) is calculated from the −1000 k/log e slope. The cross section is $y_{offset} = \log A_n\sigma_n$ where σ_n is defined as follows:

$$\frac{1}{A_n}10^{y_{offset}} = \frac{h^3}{4\sqrt{6}\pi^{\frac{3}{2}}k^2m_n^*}10^{y_{offset}}. \qquad (2)$$

When the rate window was 4.06009 s^{-1}, the activation energy and the capture cross section of signal A are obtained to be about 0.78 eV and 2.21×10^{-9} cm^{-2}, respectively.[17–19] Before considering the origin of signal A, we determined that the oxygen vacancies, titanium vacancies, and titanium interstitials on the TiO_2 NP surface and at the interface were formed by chemical reactions. According to the notation of Kröger-Vink, the formation of intrinsic point defects in TiO_2 NPs can be represented by chemical reactions between the TiO_2 and oxygen according to the following four relations:

$$O_o^x \rightleftarrows V_o^{\cdot\cdot} + 2e' + \frac{1}{2}O_2, \qquad (3)$$

$$2O_o^x + Ti_{Ti}^x \rightleftarrows Ti_i^{\cdot\cdot\cdot\cdot} + 3e' + O_2, \qquad (4)$$

$$2O_o^x + Ti_{Ti}^x \rightleftarrows Ti_i^{\cdot\cdot\cdot\cdot} + 4e' + O_2, \qquad (5)$$

$$O_2 \rightleftarrows 2O_o^x + V_{Ti}^{''''} + 4h^{\cdot}, \qquad (6)$$

where $V_{Ti}^{''''}$, $Ti_i^{\cdot\cdot\cdot}$, $Ti_i^{\cdot\cdot\cdot\cdot}$ and $V_o^{\cdot\cdot}$ are titanium vacancies, Ti_i^{3+} ions in interstitial sites, Ti_i^{4+} ions in interstitial site and oxygen vacancies, respectively. The energy levels of point defects within the energy band of TiO_2 have been reported to be about $V_o^{\cdot\cdot}$ ($E_c - 0.89$ eV, $E_c - 1.18$ eV), $Ti_i^{\cdot\cdot\cdot\cdot}$ ($E_c - 0.78$ eV), $Ti_i^{\cdot\cdot\cdot}$ ($E_c - 1.47$ eV), and $V_{Ti}^{''''}$ ($E_v + 1.15$ eV, $E_v + 1.44$ eV).[20,21] According to the results from the Arrhenius plot in Fig. 4, the activation energy was 0.78 eV, which seems to correspond to the $Ti_i^{\cdot\cdot\cdot\cdot}$ titanium vacancy. However, no signals for TiO_2 NPs in the DLTS spectra in Fig. 3 were observed. As such, the origin of this state was generally assumed to be the interface state between the TiO_2 NPs and the Sb_2S_3 QDs. One possible reason for an interfacial origin of the interface state might be the combination of lattice mismatch and dangling band effects through ionization after a chemical reaction between $Ti + O_2$ and $Sb_2 + S_3$.

Therefore, the interface states may reduce the external quantum efficiency in the solar cell device, since they affect the recombination of photo-generated electrons and holes in Sb_2S_3 semiconductor QDs. Furthermore, the interface trap densities of the measured voltage at −1 V and −2 V were approximately 2.5×10^{17} cm^{-3} and 1.4×10^{17} cm^{-3}, respectively.[22] If the measured voltages were changed from −1 V to −2 V in the Sb_2S_3 thin film or bulk semiconductors, the depth profile of the density defect states was circumscribed by measured voltages, which were able to confine the depletion width from the surface of the Au Schottky contact.[23] However, the DLTS spectra only showed the surface state between TiO_2 NPs and Sb_2S_3 QDs that occurred as a result of the screening effect at the Debye-Hückel length for nano-sized Sb_2S_3 QDs uniformly distributed on the surface of TiO_2 NPs. Therefore, even if the measurement voltages were changed from −2 V to −1 V, the interface density of states was estimated to be about $1.4 \sim 2.5 \times 10^{17}$ cm^{-3} according to the trap concentration equation. This is consistent with the definition of the DLTS signal peak and the 1×10^{18} cm^{-3} intrinsic carrier concentration for Sb_2S_3 QDs. Also, the reason for the fluctuation in density of the surface states could originate from the quantized surface state occupied by carriers.

Figure 5(a) represents the energy band diagram of Au Schottky contact/Sb_2S_3 QDs/TiO_2 NPs/FTO layer/glass substrate samples. The interface defect states should occur as a result of a chemical reaction between TiO_2 NPs and oxygen in the atmosphere or other materials. Interface states between TiO_2 NPs and Sb_2S_3 QDs were generally created as a result

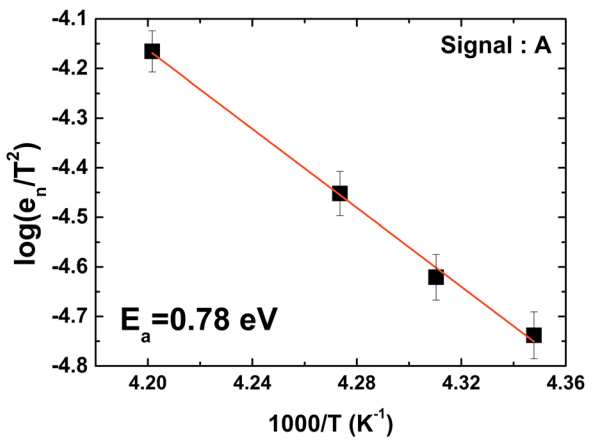

FIG. 4. Arrhenius plot of the DLTS signal measured from the sample with Sb_2S_3 QDs/TiO_2 NPs/FTO layer/glass substrate. Here, the measuring and pulse voltages were −2.0 V and 0 V, respectively.

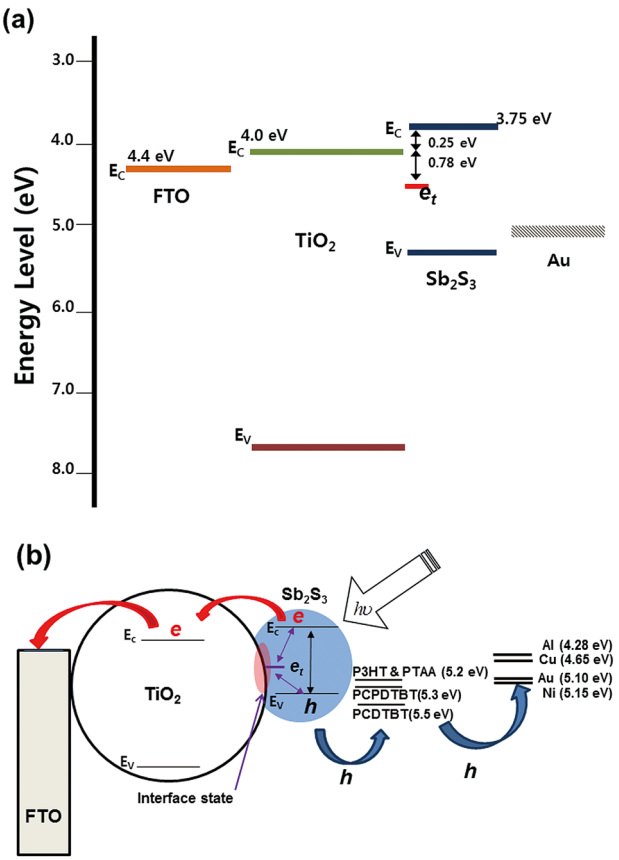

FIG. 5. (a) Energy band diagram of a Schottky Au contact/Sb_2S_3 QDs/TiO_2 NP that illustrates the emission process of electrons from defect state. Here, C_B, V_B, E_F, and e_t are the conduction band, the valance band, the Fermi energy level, and the interface trap, respectively. (b) An illustration of carrier transport from the Sb_2S_3 QDs to the FTO electrode and carrier capture process into the defect state in the inorganic-organic heterojunction Sb_2S_3 QD solar cell.

of the mismatch of the lattice structure, chemical reactions through oxygen ions, dangling bonds, and other unknown reasons. In this case, the interface states between the Au Schottky contact and Sb_2S_3 QDs did not appear in the DLTS spectra when the pulse bias was applied over 0 V in the region of minimized depletion (supplemental information.[24] However, after a filling pulse bias applied at 0 V from the Au Schottky contact to the Sb_2S_3 QDs/TiO_2 NPs, captured electrons in the surface state were emitted from the interface state in the Sb_2S_3 QDs to the conduction band (E_c) of TiO_2 NPs. Nevertheless, the activation energy of the interface state was found to be about 0.78 eV. Thus, the band-off of the E_c between TiO_2 NPs and Sb_2S_3 QDs was about 0.25 eV.[25,26] Therefore, an accurate energy level of the interface state in Sb_2S_3 was approximately $E_c - 1.03$ eV, as shown in Fig. 5(a). If photons were irradiated onto the Sb_2S_3 QDs/TiO_2 NPs solar cell, excitons in Sb_2S_3 QDs were immediately generated by an absorbed photon. Then, electrons and holes were subsequently separated from excitons that were able to transport from Sb_2S_3 QDs to the electrode through a relatively lower E_c (electron) or higher E_v (hole), as shown in Fig. 5(b). In our previous study, we demonstrated an Sb_2S_3 QDs solar cell using p-type hole-transporting materials (HTMs), such as a poly(3-hexylthiophene) (P3HT), poly[2,1,3-benzothiadiazole-4,7-diyl[4,4-bis(2-ethylhexyl)-4H-cyclopenta[2,1-b:3,4-b′]dithiophene-2,6-diyl]] (PCPDTBT), poly[[9-(1-octylnonyl)-9H-carbazole-2,7-diyl]-2,5-thiophenediyl-2,1,3-benzothiadiazole-4,7-diyl-2,5-thiophenediyl] (PCDTBT), and poly(triarylamine) (PTAA), where the positions of highest occupied molecular orbital (HOMO) were 5.2 eV, 5.3 eV, 5.5 eV, and 5.2 eV, respectively. In this work, the alignment of energy level between HOMO and HTMs for hole transfer from Sb_2S_3 QDs to metal electrodes was important for enhancing conversion efficiency of organic-inorganic Sb_2S_3 QDs solar cells.[27–31] Nevertheless, Žídek *et al.* reported a principle for improving the conversion efficiency through ultrafast transient dynamic of multiple excitons in semiconductor QDs.[32] Therefore, the carrier recombination time of the interface state in the Sb_2S_3 QDs was faster than the carrier injection times from semiconductor QDs to electrode or HTMs. The reduction in external quantum efficiency is due to an increase in resistance in circuits of QDs solar cells that occur as a result of the carrier recombinations.[33–35] Thus, interface states should be considered before demonstrating a heterojunction semiconductor QD solar cell through alignment of energy levels among QDs, HTMs, and the electrode.

In summary, the interface state between the Sb_2S_3 QDs and TiO_2 NPs of the organic-inorganic heterojunction semiconductor QD solar cell was studied using the DLTS method. The activation energy and the capture cross-section were found to be around 0.78 eV and 2.21×10^{-9} cm^{-2}, respectively. The interface state can affect the external quantum effect of the Sb_2S_3 QD solar cell because of carrier recombination at the interface state between TiO_2 NPs and Sb_2S_3 QDs. Therefore, the interface state $E_c - 1.03$ eV below the conduction band edge of Sb_2S_3 QDs should be considered to improve the external quantum efficiency of organic-inorganic hybrid semiconductor QD solar cells.

This study was supported in part by the 2012 Energy Technology Development Program funded by the Ministry of Trade, Industry and Energy (MOTIE), and the Basic Science Research Program and the Converging Research Center Program through the National Research Foundation of Korea (NRF) funded by the Ministry of Science, ICT & Future Planning (Nos. NRF-2011-0012006 and 2012K001280).

[1]R. Vogel, P. Hoyer, and H. Weller, J. Phys. Chem. **98**, 3183 (1994).
[2]O. Savadogo and K. C. Mandalm, Appl. Phys. Lett. **63**, 228 (1993).
[3]C. P. Liu, Z. H. Chen, H. E. Wang, S. K. Jha, W. J. Zhang, I. Bello, and J. A. Zapien, Appl. Phys. Lett. **100**, 243102 (2012).
[4]D. U. Lee, T. H. Lee, E. K. Kim, and I. K. Han, in *23rd European Photovoltaic Solar Energy Conference Proceeding* (EU PVSEC, Valencia, Spain, 2008), p. 633.
[5]J. W. Kiel, A. P. R. Eberle, and M. E. Mackay, Phys. Rev. Lett. **105**, 168701 (2010).
[6]S. P. Kim, D. U. Lee, and E. K. Kim, Curr. Appl. Phys. **10**, S478 (2010).
[7]P. V. Kamat, J. Phys. Chem. C **112**, 18737 (2008).
[8]A. Mellor, A. Luque, I. Tobías, and A. Martí, Appl. Phys. Lett. **101**, 133909 (2012).
[9]J. Wu, Y. F. Makableh, R. Vasan, M. O. Manasreh, B. Liang, C. J. Reyner, and D. L. Huffaker, Appl. Phys. Lett. **100**, 051907 (2012).
[10]P. K. Santra and P. V. Kamat, J. Am. Chem. Soc. **135**, 877 (2013).
[11]V. R. Reddy, J. Wu, and M. O. Manasreh, Mater. Lett. **92**, 296 (2013).
[12]S. Ito, T. N. Murakami, P. Comte, P. Liska, C. Grätzel, M. K. Nazeeruddin, and M. Grätzel, Thin Sold Films **516**, 4613 (2008).

[13]S. Messina, M. T. S. Nair, and P. K. Nair, Thin Solid Films **515**, 5777 (2007).
[14]F. C. Krebs, *Polymer Photovoltaics A Practical Approach* (SPIE, Washington, 2008), p. 43.
[15]V. Surbramanian, E. E. Wolf, and P. V. Kamat, J. Am. Chem. Soc. **126**, 4943 (2004).
[16]M. Jakob, H. Levanon, and P. V. Kamat, Nano Lett. **3**, 353 (2003).
[17]D. V. Lang, J. Appl. Phys. **45**, 3023 (1974).
[18]D. U. Lee, E. K. Kim, B. C. Lee, and D. K. Oh, Thin Solid Films **516**, 3482 (2008).
[19]L. Ha, D. U. Lee, J. S. Kim, E. K. Kim, B. C. Lee, D. K. Oh, S.-B. Bae, and K.-S. Lee, Jpn. J. Appl. Phys. Part 1 **47**, 6867 (2008).
[20]J. Nowtny, *Oxide Semiconductors for Solar Energy Conversion Titanium Dioxide* (CRC Press, Boca Raton, 2012), p. 165.
[21]M. K. Nowotny, L. R. Sheppard, T. Bak, and J. Nowotny, J. Phys. Chem. C **112**, 5275 (2008).
[22]P. Blood and J. W. Orton, *The Electrical Characterization of Semiconductor: Majority Carriers and Electron States*, (Academic Press, London, 1992), p. 351.
[23]M. Kaniewska, O. Engström, A. Barcz, and M. Pacholak-Cybulska, Mater. Sci. Eng., C **26**, 871 (2006).
[24]See supplementary material at http://dx.doi.org/10.1063/1.4813272 for the DLTS spectra of pulse voltage at 1 V.
[25]P. P. Boix, G. Larramona, A. Jacob, B. Delatouche, I. Mora-Seró, and J. Bisquert, J. Phys. Chem. C **116**, 1579 (2012).
[26]D. Kieven, A. Grimm, I. Lauermann, T. Rissom, and R. Klenk, Appl. Phys. Lett. **96**, 262101 (2010).
[27]J. A. Chang, J. H. Rhee, S. H. Im, Y. H. Lee, H.-J. Kim, S. I. Seok, M. K. Nazeeruddin, and M. Gratzel, Nano Lett. **10**, 2609 (2010).
[28]S. H. Im, C.-S. Lim, J. A. Chang, Y. H. Lee, N. Maiti, H.-J. Kim, M. K. Nazeeruddin, M. Grätzel, and S. I. Seok, Nano Lett. **11**, 4789 (2011).
[29]J. A. Chang, S. H. Im, Y. H. Lee, H.-J. Kim, C.-S. Lim, J. H. Heo, and S. I. Seok, Nano Lett. **12**, 1863 (2012).
[30]J. H. Noh, S. H. Im, J. H. Heo, T. N. Mandal, and S. I. Seok, Nano Lett. **13**, 1764 (2013).
[31]J. H. Heo, S. H. Im, J. H. Noh, T. N. Mandal, C.-S. Lim, J. A. Chang, Y. H. Lee, H. Kim, A. Sarkar, M. K. Nazeeruddin, M. Grätzel, and S. I. Seok, Nat. Photonics **7**, 486 (2013).
[32]K. Žídek, K. Zheng, M. Abdellah, N. Lenngren, P. Chábera, and T. Pullerits, Nano Lett. **12**, 6393 (2012).
[33]R. J. Ellingson, M. C. Beard, J. C. Johnson, P. Yu, O. I. Micic, A. J. Nozik, A. Shabaev, and A. L. Efros, Nano Lett. **5**, 865 (2005).
[34]J. Nelson, *The Physics of Solar Cells* (Imperial College Press, London, 2003), p. 110.
[35]P. P. Boix, G. Larramona, A. Jacob, B. Delatouche, I. Mora-Seró, and J. Bisquert, J. Phys. Chem. C **116**, 1579 (2012).